Self-induced density modulations in the free expansion of Bose-Einstein condensates

Luca Salasnich,[1] Nicola Manini,[2,3] Federico Bonelli,[2] Michael Korbman,[2] and Alberto Parola[4]
[1]*CNISM and CNR-INFM, Unità di Padova, Dipartimento di Fisica "Galileo Galilei," Università di Padova, Via Marzolo 8, 35131 Padova, Italy*
[2]*Dipartimento di Fisica, Università di Milano, Via Celoria 16, 20133 Milano, Italy*
[3]*CNISM, Unità di Milano, Via Celoria 16, 20133 Milano, Italy*
[4]*Dipartimento di Fisica e Matematica, Università dell'Insubria, Via Valleggio 11, 22100 Como, Italy*
(Received 12 January 2007; revised manuscript received 9 March 2007; published 19 April 2007)

We simulate numerically the free expansion of a repulsive Bose-Einstein condensate with an initially Gaussian density profile. We find a self-similar expansion only for weak interatomic repulsion. In contrast, for strong repulsion we observe the spontaneous formation of a shock wave at the surface followed by a significant depletion inside the cloud. In the expansion, contrary to the case of a classical viscous gas, the quantum fluid can generate radial rarefaction density waves with several minima and maxima. These intriguing nonlinear effects, never observed in free-expansion experiments with ultracold alkali-metal atoms, can be detected with the available setups.

DOI: 10.1103/PhysRevA.75.043616 PACS number(s): 03.75.Ss, 03.75.Hh, 64.75.+g

I. INTRODUCTION

The anisotropic free expansion of a gas of ^{87}Rb atoms was the first experimental evidence of Bose-Einstein condensation in ultracold gases [1]. The nonballistic free expansion observed with ^{6}Li atoms has been saluted as the first signature of superfluid behavior in an ultracold Fermi vapor [2]. In both cases the atomic quantum gases can be described by the hydrodynamic equations of superfluids and, because the initial density profile is an inverted parabola, the free expansion is self-similar [3–7].

The first theoretical investigations of the free expansion into vacuum of a classical gas sphere with constant initial density date back to the 1960s [8,9]: Numerical analysis was needed to analyze in detail the formation of a depletion at the center and of a shock wave at the surface [10,11]. More recently, rarefaction waves have been produced experimentally by the free expansion of an electron plasma [12].

In the present work we investigate the intriguing nonlinear phenomena that the free expansion of a bosonic superfluid into vacuum displays. In particular, by integrating numerically [13] the time-dependent Gross-Pitaevskii equation (GPE) [14] we show that the expansion of a repulsive Bose-Einstein condensate (BEC) of initial Gaussian density profile gives rise to central depletion and self-induced density modulations, i.e., self-induced rarefaction waves. In addition, we find that the expanding cloud produces a shock wave at the surface, that is regularized by the quantum pressure of the superfluid. Similar nonlinear effects were investigated in the past in different conditions. In particular, Zak [15] and Damski [16] analyzed the 1D nonlinear evolution and the nondissipative shock waves induced by density perturbations of BEC's. Kamchatnov and collaborators [17] studied the shock-wave formation and regularization in the propagation of a 2D density perturbation over a uniform background. Pérez-García *et al.* [18] investigated the shock-wave formation induced by the rapid increase of the scattering length in a trapped BEC. Ruschhaupt and collaborators [19] investigated the early times of the expansion of 1D and 3D (spherically symmetric) Gaussian-shaped BEC packets, from the perspective of velocity distribution. The general understanding is that, while shock waves occur in all space dimensions, the central depletion is characteristic of 3D expansion.

Shock and rarefaction waves induced by a density perturbation were observed recently in BEC's [20,21] and also in nondissipative nonlinear optics [22]. In the present work we propose an experiment well within the present-day technological capability: By exploiting the Fano-Feshback resonance mechanism [23] tuned by an external magnetic field, it is possible to equilibrate a trapped BEC characterized by a very small scattering length, thus producing a stationary Gaussian density profile, and then simultaneously remove the confining trap and change the magnetic field, making the scattering length very large, thus initiating the expansion of an initially-Gaussian strongly interacting expanding BEC. We illustrate the depletion and shock phenomena that should be observed in such kind of experiments.

II. THE NUMERICAL EXPERIMENT

We describe the collective motion of the BEC of N atoms in terms of a complex mean-field wave function $\psi(\mathbf{r},t)$ normalized to unity and such that $\rho(\mathbf{r},t)=N\rho_1(\mathbf{r},t)=N|\psi(\mathbf{r},t)|^2$ is the number-density distribution. The equation of motion that we assume for $\psi(\mathbf{r},t)$ is the time-dependent GPE [14]

$$i\hbar\frac{\partial}{\partial t}\psi=\left[-\frac{\hbar^2}{2m}\nabla^2+U+\frac{4\pi\hbar^2 a_s}{m}N|\psi|^2\right]\psi, \qquad (1)$$

where $U(\mathbf{r},t)$ is a confining potential that we assume to vanish at $t\geq 0$ (thus allowing free expansion) and m is the atomic mass. The nonlinear term represents the interatomic interaction at a mean-field level, where a_s is the s-wave scattering length, and we consider the repulsive regime $a_s>0$.

In traditional experiments with ultracold alkali-metal atoms [1,2] expansion starts from an initial state coinciding with the ground state of the confined superfluid under the action of a (often anisotropic) harmonic potential. For robust

interparticle interaction (large number of particles), the density profile in this initial state resembles closely a negative-curvature parabola [14]. When such density profile is taken as the initial state of a successive free nonballistic expansion, to a very good degree of approximation it expands in a self-similar fashion, maintaining the same shape and only spreading out and scaling down its height proportionally, until a ballistic regime is reached when dilution leads to a fully noninteracting regime [3–7].

In the present work we discuss the much more exciting phenomena observed in the expansion of an interacting condensate starting off as a stationary Gaussian

$$\psi(\mathbf{r},0)=\frac{1}{(\pi\sigma^2)^{3/4}}\exp\left(-\sum_{i=x,y,z}\frac{r_i^2}{2\sigma_i^2}\right), \tag{2}$$

with $\sigma^3=\sigma_x\sigma_y\sigma_z$. Note that a Gaussian profile is readily achieved experimentally by equilibrating the BEC with a very small scattering length a_s obtained by means of the Fano-Feshbach resonance technique [14,23] with a carefully tuned external constant magnetic field. a_s can then be set to the desired value by a sudden change in the magnetic field at the time when the harmonic trapping potential is switched off.

The isotropic case $\sigma_x=\sigma_y=\sigma_z=\sigma$ is conceptually advantageous, as the expansion can be studied within the GPE model in its full generality as a function of a single parameter. Consider rescaling the variables of Eq. (1) as follows: $\mathbf{r}\to\mathbf{r}/\sigma$, $t\to t\hbar/(m\sigma^2)$, and $\psi\to\psi\sigma^{3/2}$, to produce a dimensionless form

$$i\frac{\partial}{\partial t}\psi=\left[-\frac{1}{2}\nabla^2+g|\psi|^2\right]\psi, \tag{3}$$

of the equation for the free expansion of a condensate expansion starting off from a Gaussian initial state of unit width. The dimensionless interaction strength $g=4\pi Na_s/\sigma$ is the one free parameter determining the properties of the free expansion. The scattering length of ^{23}Na atoms can be increased to $a_s\simeq 10$ nm, thus producing $g\simeq 10^4$ for BEC's of $N\simeq 10^5$ in current traps of frequency $\simeq 1000$ Hz [25].

We simulate the expansion experiment numerically by using an efficient finite-difference Crank-Nicolson algorithm [13]: We verify that little changes affect the expansion as long as the interaction is small. $g<1$ tracks the weak-coupling limit where interaction only accelerates slightly the free expansion described by

$$\psi(\mathbf{r},t)=\frac{1}{\pi^{3/2}(1+t^2)^{3/2}}\exp\left(-\frac{r^2(1+it)}{2(1+t^2)}\right) \tag{4}$$

[24], while $g\gg 1$ represents the strong-coupling regime, where the mean-field self-interaction term in Eq. (3) dominates the expansion for long enough to produce substantial nonlinear effects such as those sketched in Fig. 1. In particular we observe the rapid buildup of a sharp expanding spherical density wave which leaves behind a central region of depleted density. New successively formed radial ripples cross this density-depleted region. Eventually, at very long times, when the overall density has decayed enough for the nonlinear term in Eq. (3) to become negligible everywhere, the expansion recovers a bell-shaped profile.

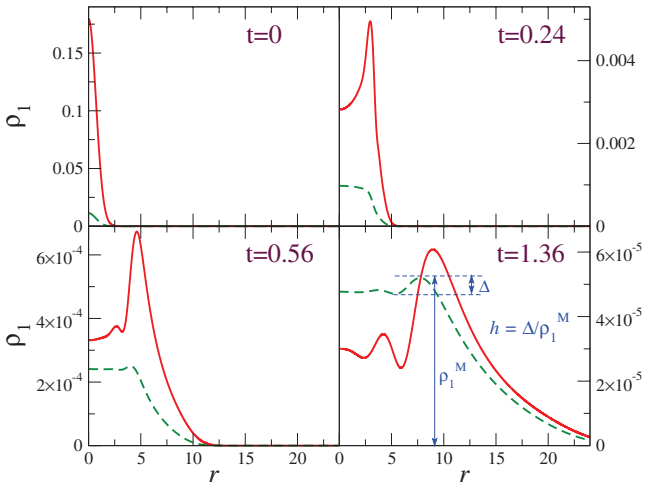

FIG. 1. (Color online) Four successive frames of the radial density profile (solid line) for the expansion of a strongly interacting condensate, characterized by dimensionless interaction parameter $g=2000$. The "opacity" of the expanding cloud (dashed line) given by the density $\rho_1(\mathbf{r})$ integrated along lines at a distance r from the center (rescaled by a factor 0.036). All quantities are dimensionless: Lengths in units of the initial Gaussian width σ and time in units of $m\sigma^2/\hbar$.

More quantitatively, for increasing g, the rarefaction starts to be evidenced by a local minimum at the droplet center for $g\gtrsim 48.3$, and becomes more and more pronounced and long lived for larger interaction strength g. In the highly nonlinear regime, the free expansion of the bosonic cloud into vacuum develops sequences of radial density waves with minima and maxima, each starting at a characteristic time and disappearing at a later time. Figure 2 tracks a few early times in this class, as a function of g: More could be defined for larger g. Overall, the time $t_{\rm am}$ of appearance of the first local minimum reduces slowly as g increases, while the time $t_{\rm dm}$ of disappearance of all local minima and recovery of a bell-shaped profile increases rapidly with g. In between these two characteristic times several traveling density minima and maxima can be formed depending on the value of g. Generally, the number and density difference of local minima and maxima increases with the interaction strength.

In practice, the visibility of the central depletion need not be easy to appreciate by means of total opacity measurements, since such measurements address the integrated density of a generic linear section crossing the droplet at a given distance from its center. However, Fig. 1 shows that for suitably strong interaction, a sensibly higher-opacity outer ring does indeed develop. The inset of Fig. 2 tracks the time range when this inner optical-density minimum remains lower than the outside denser ring by at least 1% and 5%: It is seen that for strong enough interaction ($g\gtrsim 215$ and $g\gtrsim 310$, respectively), the depleted region realizes a limited but significant visibility, which improves for stronger coupling. An example of visible opacity ring is displayed in the upper right corner of Fig. 2.

To characterize the dynamics of the bosonic cloud it is useful to introduce its local phase velocity, given by

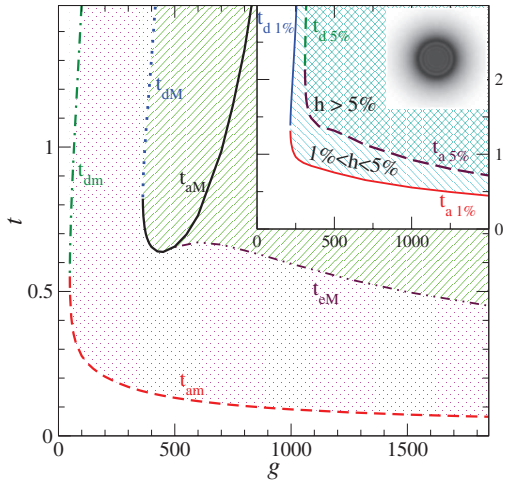

FIG. 2. (Color online) Characteristic times of the free expansion as a function of the interaction strength g. For $g \geqslant 48.7$, a first minimum in the radial density profile appears at the center $r=0$ at time t_{am} (dashed) and fills in at t_{dm} (dot-dashed). For $g \geqslant 363$, a local maximum reforms at the center at time t_{aM} (solid) and disappears at time t_{dM}. A density maximum appears within the rarefaction region at time t_{eM} (dot-dot-dashed). Inset: The time of appearance t_a and disappearance t_d of a denser ring (sketched in the small square for $g=1200$ and $t=1.8$) of visibility h (defined in Fig. 1) 1% (solid) and 5% (dashed) in the opacity profile (dashed lines of Fig. 1), as a function of g. Units as in Fig. 1.

$$\mathbf{v} = \frac{i}{2}\frac{\psi \nabla \psi^* - \psi^* \nabla \psi}{|\psi|^2}. \tag{5}$$

This velocity can be written as $\mathbf{v}(\mathbf{r},t)=\nabla\theta(\mathbf{r},t)$, where $\theta(\mathbf{r},t)$ is the phase of the macroscopic wave function $\psi(\mathbf{r},t)=\rho_1(\mathbf{r},t)^{1/2}e^{i\theta(\mathbf{r},t)}$ of the bosonic superfluid. From Eq. (4) one finds immediately the radial phase velocity of a spherical noninteracting Bose gas ($g=0$):

$$v = \frac{r}{2}\frac{t}{1+t^2}. \tag{6}$$

In the interacting case ($g>0$) the nonlinear term acts as the chemical potential of a fluid of classical pressure $P=g|\psi|^4/2$ and sound velocity $c_s=\sqrt{g|\psi|^2}$ [14]. For $g \ll 1$ the gas velocity follows Eq. (6) closely, while for large g deviations from Eq. (6) are substantial, as mainly the interaction term, rather than the quantum tendency to delocalization, drives the expansion. The ratio v/r, a constant as a function of r according to Eq. (6) in a noninteracting expansion, shows strong deviations induced by the nonlinear term $g|\psi|^2$. In practice, the phase velocity of a strongly interacting BEC approaches the local sound velocity, with larger densities implying higher velocities. Accordingly, initially the central part of the strongly repulsive bosonic superfluid accelerates and propagates faster than the periferic part: The ensuing mass flow is responsible for the formation of the rarefaction region inside the cloud, shown in Fig. 1. The matter flowing quickly out of the central region accumulates near the profile edge on top of the slower external tail, thus tending to produce a shock wave [16–18,21,22], with a BEC density profile extremely steep at the surface, approaching a step function: This is illustrated by the $t=0.24$ panel of Fig. 1. This steep wave front survives for a brief period, after which density oscillations shoot backwards and the surface profile rapidly smoothens its density gradient. At this point, the expansion dynamics is strongly affected by these backward density oscillations, which induce a *inverted* relation between local velocity and density, as Fig. 3 illustrates: For a strongly interacting BEC, at a fixed time t the ratio v/r finds local maxima (minima) in correspondence to the local minima (maxima) of the density profile ρ_1. This inversion demonstrates the *inward* motion of the density ripples. These local minima represent the rarefaction waves produced by the surface step smoothing. This smoothing is driven by the quantum pressure term [16].

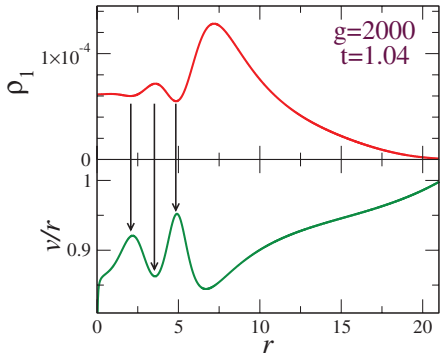

FIG. 3. (Color online) Comparison of the density profile $\rho_1(r)=|\psi(r)|^2$ and of the velocity profile $v(r)/r$ for the spherically symmetrical expansion of the strongly interacting bosonic cloud. Units as in Fig. 1.

III. COMPARISON TO CLASSICAL HYDRODYNAMICS

The quantum pressure $-(|\nabla\psi|^2)/(2\rho_1)$, which plays a negligible role in the self-similar nonballistic expansion [7] of both Fermi and Bose superfluids with an inverted-parabola initial profile [26], becomes relevant in regularizing the shock-wave singularity, like the dissipative term in classical hydrodynamics [21]. Analogous depletion and shock-wave phenomena are indeed observed in the hydrodynamical expansion of hot classical fluids, and can be simulated, e.g., by means of the Navier-Stokes equations (NSE), which depend on the (dissipative) coefficient of shear viscosity η [9]. For $\eta=0$ the irrotational ($\nabla\wedge\mathbf{v}=\mathbf{0}$) NSE reduce to the Euler equations of an ideal (nonviscous) fluid. By using $P(\rho)=g\rho_1^2/2$ as the equation of state, the Euler equations are exactly equivalent to the GPE without the quantum pressure term [14]. In Fig. 4 we compare the expanding BEC [GPE, Eq. (3)] and classical gas (NSE), for $g=10000$. The NSE are solved by means of a Lagrangian finite-difference method [27]. The four successive frames displayed in Fig. 4 show that, while expanding, the interacting BEC and the classical gas produce a remarkably similar self-depletion of the central region. On the other hand, the multipeak rarefaction structures predicted by the GPE are not reproduced by the NSE. Thus the novelty of the free expansion of a BEC with respect

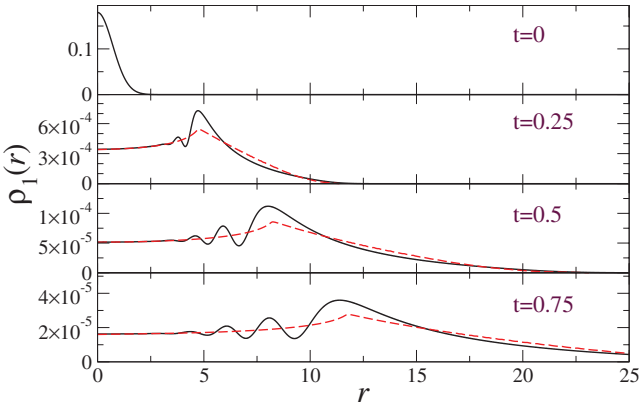

FIG. 4. (Color online) Self-depleting radial density profile $\rho_1 = \rho/N$ during the expansion: Comparison between the strongly interacting Bose gas (GPE, solid lines) and the classical gas (NSE, dashed lines), with $g=1^4$ and the same initial conditions (a unit Gaussian). In the NSE, the shear viscosity coefficient $\eta=10^{-5}$. Units as in Fig. 1.

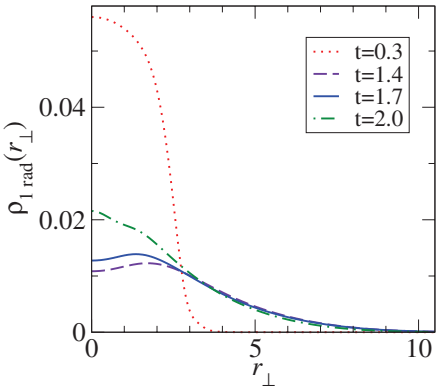

FIG. 5. (Color online) Successive frames of the expansion of the radial density $\rho_{1\mathrm{rad}}(r_\perp) \equiv \int_\infty^\infty \rho_1(r_\perp, z)dz$, obtained starting from an isotropic Gaussian wave packet of unit width, for dimensionless interaction $g=500$ and radial confinement of unit frequency $\omega_\perp = 1$.

to that of a weakly viscous classical fluid, stands mainly in the distinct large-amplitude rarefaction waves moving inside the depletion region, which are supported by the nondissipative nature of quantum pressure.

IV. DISCUSSION OF THE ROLE OF DIMENSIONALITY

The expansion of the BEC in an anisotropic context is also instructive. In particular, we find that a one-dimensional (1D) expansion starting from a Gaussian state produces no central depletion. Interestingly, Ruschhaupt *et al.* [19] demonstrate a depletion even in 1D, by switching the interaction off after a brief time interval. By leaving the interaction on at all times instead, we find no central depletion whether we examine an ideally 1D BEC, represented by a purely 1D GPE, or when we simulate the 3D expansion of a Gaussian wavepacket to which an harmonic confining potential is kept along two orthogonal space directions at all times, with free expansion being allowed along a single direction z. In both geometries shock-wave phenomena arise along the axial direction, as previously shown by Damski in the strictly 1D geometry [16]. In the detail, in the latter cylindrical geometry, if we take a spherical Gaussian (2) of width equal to the confining-potential harmonic length $[\hbar/(m\omega_\perp)]^{1/2}$ as the initial state, the strongly interacting BEC initially shoots out rapidly in all directions, including the confined ones, thus producing shock, depletion, and rarefaction waves around the cylindrical-symmetry axis. Figure 5 illustrates this rapid initial expansion and depletion (dotted and dashed profiles), driven by interaction, followed by a return toward the cylinder axis induced by the confining potential (solid and dot-dashed profiles). Likewise, along the z axis the density does show a depletion in a suitable time interval, but the integrated density $\rho_{1\mathrm{ax}}(z) \equiv 2\pi \int_0^\infty \rho_1(r_\perp, z) r_\perp dr_\perp$ retains a bell shape at all times, even for very large interaction, thus confirming the qualitative behavior of the purely 1D model.

In conclusion, we show that the free expansion of a BEC reveals novel and interesting nonlinear effects, including radial rarefaction density waves with several minima and maxima not achievable with classical viscous fluids, and which are awaiting experimental investigations.

ACKNOWLEDGMENTS

The authors thank Paolo Di Trapani, Luciano Reatto, and Flavio Toigo for useful suggestions.

[1] M. H. Anderson *et al.*, Science **269**, 198 (1995).
[2] K. M. O'Hara, S. L. Hemmer, M. E. Gehm, S. R. Granade, and J. E. Thomas, Science **298**, 2179 (2002).
[3] Y. Castin and R. Dum, Phys. Rev. Lett. **77**, 5315 (1996).
[4] Yu. Kagan, E. L. Surkov, and G. V. Shlyapnikov, Phys. Rev. A **54**, R1753 (1996); **55**, R18 (1997).
[5] P. Öhberg and L. Santos, Phys. Rev. Lett. **89**, 240402 (2002).
[6] L. Salasnich, A. Parola, and L. Reatto, Phys. Rev. A **72**, 025602 (2005).
[7] G. Diana, N. Manini, and L. Salasnich, Phys. Rev. A **73**, 065601 (2006).
[8] P. Molmud, Phys. Fluids **3**, 362 (1960).
[9] Ya. B. Zel'dovich and Yu. P. Raizer, *Physics of Shock Waves and High-Temperature Hydrodynamic Phenomena* (Dover Publications, Mineola, NY, 2002) [in Russian, (Izd. Nauka, Moscow 1966)].
[10] V. E. Kondrashov, A. N. Polyanichev, and V. S. Fetisov, Fluid Dyn. **9**, 835 (1974).
[11] N. C. Freeman and S. Kumar, J. Fluid Mech. **56**, 523 (1972); N. C. Freeman, R. S. Johnson, S. Kumar, and W. B. Buch, *ibid.* **68**, 625 (1975).
[12] J. D. Moody and C. F. Driscoli, Phys. Plasmas **2**, 4482 (1995).

[13] E. Cerboneschi, R. Mannella, E. Arimondo, and L. Salasnich, Phys. Lett. A **249**, 495 (1998); L. Salasnich, A. Parola, and L. Reatto, Phys. Rev. A **64**, 023601 (2001).
[14] L. P. Pitaevskii and S. Stringari, *Bose-Einstein Condensation* (Oxford University Press, Oxford, 2003).
[15] M. Zak and I. Kulikov, Phys. Lett. A **307**, 99 (2003); I. Kulikov and M. Zak, Phys. Rev. A **67**, 063605 (2003).
[16] B. Damski, Phys. Rev. A **69**, 043610 (2004); **73**, 043601 (2006).
[17] A. M. Kamchatnov, A. Gammal, and R. A. Kraenkel, Phys. Rev. A **69**, 063605 (2004).
[18] V. M. Pérez-García, V. V. Konotop, and V. A. Brazhnyi, Phys. Rev. Lett. **92**, 220403 (2004).
[19] A. Ruschhaupt, A. del Campo, and J. G. Muga, Eur. Phys. J. D **40**, 399 (2006).
[20] Z. Dutton, M. Budde, C. Slowe, and L. V. Hau, Science **293**, 663 (2001).
[21] M. A. Hoefer, M. J. Ablowitz, I. Coddington, E. A. Cornell, P. Engels, and V. Schweikhard, Phys. Rev. A **74**, 023623 (2006).
[22] W. Wan, S. Jia, and J. W. Fleischer, Nat. Phys. **3**, 46 (2007).
[23] U. Fano, Nuovo Cimento **12**, 156 (1935); H. Feshbach, Ann. Phys. (N.Y.) **5**, 357 (1958); U. Fano, Phys. Rev. **124**, 1866 (1961).
[24] R. Robinett, *Quantum Mechanics. Classical Results, Modern Systems, and Visualized Examples* (Oxford University Press, Oxford, 2006).
[25] J. Stenger, S. Inouye, M. R. Andrews, H.-J. Miesner, D. M. Stamper-Kurn, and W. Ketterle, Phys. Rev. Lett. **82**, 2422 (1999).
[26] N. Manini and L. Salasnich, Phys. Rev. A **71**, 033625 (2005).
[27] R. D. Richtmyer and K. W. Morton, *Difference Methods for Initial-Value Problems* (Wiley, New York, 1967).